HHS Public Access

Author manuscript

Exp Eye Res. Author manuscript; available in PMC 2015 August 01.

Published in final edited form as:

Exp Eye Res. 2014 August ; 125: 173–182. doi:10.1016/j.exer.2014.06.014.

Assessment of Anti-Scarring Therapies in *Ex Vivo* Organ Cultured Rabbit Corneas

Sriniwas Sriram[1], **Daniel Gibson**[2], **Paulette Robinson**[3], **Liya Pi**[3], **Sonal Tuli**[4], **Alfred S. Lewin**[5], and **Gregory Schultz**[2]

[1]Schepens Eye Research Institute, Harvard Medical School, University of Florida

[2]Institute for Wound Research, Department of Obstetrics and Gynecology, University of Florida

[3]Department of Pediatrics, University of Florida

[4]Department of Ophthalmology, University of Florida

[5]Department of Molecular Genetics and Microbiology, University of Florida

Abstract

The effects of a triple combination of siRNAs targeting key scarring genes was assessed using an *ex vivo* organ culture model of excimer ablated rabbit corneas. The central 6 mm diameter region of fresh rabbit globes was ablated to a depth of 155 microns with an excimer laser. Corneas were excised, cultured at the air-liquid interface in defined culture medium supplemented with transforming growth factor beta 1 (TGFB1), and treated with either 1% prednisolone acetate or with 22.5 μM cationic nanoparticles complexed with a triple combination of siRNAs (NP-siRNA) targeting TGFB1, TGFB Receptor (TGFBR2) and connective tissue growth factor (CTGF). Scar formation was measured using image analysis of digital images and levels of smooth muscle actin (SMA) were assessed in ablated region of corneas using qRT-PCR and immunostaining. *Ex vivo* cultured corneas developed intense haze-like scar in the wounded areas and levels of mRNAs for pro-fibrotic genes were significantly elevated 3 to 8 fold in wounded tissue compared to unablated corneas. Treatment with NP-siRNA or steroid significantly reduced quantitative haze levels by 55% and 68%, respectively, and reduced SMA mRNA and immunohistostaining. This *ex vivo* corneal culture system reproduced key molecular patterns of corneal scarring and haze formation generated in rabbits. Treatment with NP-siRNAs targeting key scarring genes or an anti-inflammatory steroid reduced corneal haze and SMA mRNA and protein.

1. INTRODUCTION

Corneal haze is a common complication that occurs in patients after excimer laser photorefractive keratectomy (PRK).(Sakimoto et al., 2006) Mechanical, chemical and/or

Contact details – Sriniwas Sriram, PhD, Schepens Eye Research Institute, Phone: 617-912-0280, sriniwas_sriram@meei.harvard.edu, Fax: 617.912.0107.

surgical injury to the cornea triggers a complex wound healing response causing changes in extracellular matrix organization, cellular phenotype and density.(Jester et al., 1999) There is no fibrotic response in case of superficial epithelial lesions, as stem cells from either the surrounding limbus or other parts of the epithelium migrate into the wounded region and rapidly resolve the wound.(Liang et al., 2009; Pellegrini et al., 2009) However, deeper wounds disturbing the basal epithelium and stromal layers stimulate the pathological evolution of the wounding process mainly due to the involvement of fibrogenic growth factors like transforming growth factor beta 1 (TGFB1), TGFB Receptor (TGFBR2) and connective tissue growth factor (CTGF).(Blalock et al., 2003; Tandon et al., 2010) When the quiescent keratocytes come in contact with these growth factors, they decrease expression of corneal crystallins and become activated fibroblasts that begin to repopulate the stroma, replacing the resident cells that had undergone apoptosis following the injury. These activated keratocytes proliferate and rapidly synthesize extracellular matrix (ECM) including collagen molecules lack the highly structured orthogonal array pattern that is present in clear cornea. Many activated fibroblasts undergo further phenotypic changes typical of myofibroblasts.(Jester et al., 1996; Møller-Pedersen, 2004) These myofibroblasts are characterized by their high concentration of alpha smooth muscle actin (SMA) that forms intracellular scaffolding that effectively scatters light, and by elevated expression of cadherins and TGFβ1receptors.(Jester et al., 1999) Also, unlike the activated fibroblasts, the myofibroblasts typically can persist for extended periods do not apoptose as the stromal injury undergoes remodeling. The combination of loss of corneal crystallin proteins, synthesis of new ECM with irregularly arrayed collagen fibers, and the presence of larger numbers of myofibroblasts leads to the generation of corneal haze.(Eraslan and Toker, 2009)

Several *ex vivo* corneal models have reported tests for re-epithelialization after physical (Tanelian and Bisla, 1992; Carrington et al., 2006), chemical (Chuck et al., 2001a; Saghizadeh et al., 2013) and laser wounds (Janin-Manificat et al., 2012). However, most of the models are mainly concerned with the process of re-epithelialization, and only limited studies have evaluated corneal scarring by analyzing pro-fibrotic markers. In particular, none of the previous *ex vivo* models has evaluated the therapeutic potential of gene therapy in these culture models.

RNA interference (RNAi) is the process of sequence-specific post-transcriptional gene silencing triggered by double-stranded RNAs. Recent studies have suggested that long siRNAs (27–29 nucleotides) that enter the RNA interference (RNAi) pathway in a Dicer-dependent fashion provide more efficient gene silencing than shorter, Dicer-independent substrates. (Kim et al., 2005; Siolas et al., 2005) However, siRNAs of 21 nucleotides (nt) or more have been shown to induce an innate immune response stimulating many of the published effects of the siRNAs. (Reynolds et al., 2006; Kleinman et al., 2008; Grimm, 2009) Short siRNAs (19–21nt) can lower the risk of such off-target effects whilst being just as effective in knocking down the target mRNA expression. (Grimm, 2009) The siRNA sequences used in this study are 19 nt in length and have been shown to be effective in knocking down the expressions of TGFB1, TGFBR2 and CTGF mRNA expression. (sriram et al., 2013c)

It is often difficult to achieve a significant therapeutic effect by employing a one- target, one-drug paradigm for a complex, multi-factorial, amplifying, signaling pathway.(Chou and Talalay, 1983) Hence, a multi-target approach can interrupt or act on complex signaling networks at multiple points, and affect the cell in ways that an individual component cannot. It is also less vulnerable to acquired resistance as the system is less able to compensate for the action of two or more drugs simultaneously.(Borisy et al., 2003; Keith et al., 2005) In this study, we used a triple siRNA combination targeting three key scarring genes – TGFB1, TGFBR2 and CTGF. In addition to knocking down the target mRNA expressons, the triple siRNA combination was also effective in knocking down the expressions of SMA and Collagen-I in *in vitro* experiments. (sriram et al., 2013c)

The principal properties governing absorption of a drug by the cornea are the lipophilicity, partition coefficient and molecular size of that compound.(Lee and Robinson, 1986; Sasaki et al., 1996) The multi-layered corneal epithelium, which possesses extensive tight junction complexes, is generally the rate-limiting physical barrier to penetration of drugs through the cornea.(Hämäläinen et al., 1997) Similarly, endothelial cell layer also provides a substantial barrier to drug penetration. The stroma is primarily composed of large collagen fibers embedded in a proteoglycan matrix forming the bulk of the cornea. Due to its high water content (~78%), it provides minimal resistance to small hydrophilic molecules. (Edwards and Prausnitz, 2001) Other mechanisms that hinder delivery of drugs into the eye also include lacrimation and tear drainage. Hence, for an effective therapy, a delivery method to target the corneal layer with the maximum post-wounding growth factor localization has to be developed.

Nanoparticle carriers provide a potential solution for targeted ocular drug delivery, as they have been shown to be non-immunogenic, have relatively low toxicity, resistant to protein/serum absorption and stable in an enzymatic environment. Cationic nanoparticles have also been shown to adhere to the ocular surface and transfect corneal epithelial cells, after topical administration.(Tong et al., 2007; la Fuente et al., 2008) Therefore, in this study, we are tested the efficacy of a nanoparticle carrier system to deliver siRNAs to the different layers of the cornea.

Overall, these experiments characterized scar formation in an *ex vivo* rabbit corneal organ culture model following a laser ablation and compared it to that of scar formation in the rabbit animal model. We also evaluated the therapeutic potential of the model by delivering a previously optimized triple siRNA combination to the cornea and assessed its effect on scar formation.

2. METHODS

2.1 Nanoparticles

A commercially available nanoparticle kit, Invivoplex® was purchased from Aparnabio (Rockville, MD) and used according to manufacturer's instructions. Briefly, the siRNA triple combination solution was made at a concentration of 0.9 mg/ml and 600 μL of this solution was added with 300 μL of the provided cargo buffer. This solution was added drop wise to 900 μL of the nanoparticles while stirring with a magnetic stirrer. This preparation

formed siRNA containing particles of less than 50 nm that were stable for a week at 4°C with low levels of *in vivo* cytotoxicity.(Chou et al., 2011)

2.2 RNA interference

In a previous paper, we generated an effective triple siRNA combination targeting TGFB1, TGFBR2 and CTGF with high synergy among its individual siRNA sequences. (sriram et al., 2013a; 2013c) The effective triple siRNA, in *in vitro* knockdown experiments, significantly reduced mRNA levels of target genes (>80%) and downstream scarring genes (>85%), SMA protein (>95%), and significantly reduced cell migration without reducing cell viability. This previously optimized, effective, triple combination of siRNAs was tested for its efficacy in knocking down key scarring genes in this *ex vivo* corneal scarring model. In this study, siSTABLE® siRNAs, which are chemically modified to persist in *in vivo* conditions, were ordered Dharmacon (Dharmacon Products, Thermo Fisher Scientific, Lafayette, CO).

2.3 *Ex vivo* organ culture of rabbit corneas

Corneas were cultured as previously described with some important modifications.(Chuck et al., 2001b; Castro-Combs et al., 2008; Richard et al.) The ends of 50 ml laboratory test tubes were cut off at the indicator lines nearest to the bottom using a thin saw blade. The cut rim of tubes were then coated with methyl cyanoacrylate based “super glue” and aseptically pressed onto the center of each well of a 12-well tissue culture plate, creating a dome shaped support surface for corneas. Plates were then sanitized by placing them under ultraviolet light overnight. The central 6 mm diameter area of corneas of fresh rabbit globes (Pelfreeze) was ablated to a total depth of 155 microns using a Nidek excimer laser in phototherapeutic keratectomy mode, Ablated corneas were then surgically dissected from the rabbit globes using sterile scalpel and forceps, grasping only the scleral rims and not the clear cornea. Test agents were added to the media, immediately after placing the corneas on the domes. The corneas were incubated at 37° C in humidified atmosphere containing 5% CO_2 for the duration of the experiment. The level of the culture medium was adjusted so the anterior surface of corneas was at the air-liquid interface. as described below.

2.3.1 Experiment 1—Experiment 1 was designed to assess if the excimer laser ablated corneas developed patterns of gene expression that was consistent with scar formation after two weeks of organ culture. Two groups of corneas were analyzed: ablated, and unablated corneas. Four corneas were cultured in each of the two groups in DMEM supplemented with 10% fetal bovine serum containing 1% antibiotic solution (penicillin and streptomycin) and the media was changed every 2 days. After 14 days of culture, mRNA from the four corneas in each treatment group were pooled together and processed for q-RT-PCR measurement of levels of mRNAs for five genes as described below: TGFB1, TGFBR2, CTGF, SMA and Col-I.

2.3.2 Experiment 2—Experiment 2 was designed to assess the delivery of a fluorescently labeled scrambled siRNA sequence using NP (NP-FL-siRNA). The experiment included three groups of corneas: unablated & treated with NP-FL-siRNA, ablated & treated with NP-FL-siRNA and ablated & treated FL-siRNA without NP. Three corneas were cultured in

each of the three groups in DMEM supplemented with 10% fetal bovine serum containing 1% antibiotic solution (penicillin and streptomycin) and the media was changed every 2 days. The corneas in the NP-FL-siRNA group (three ablated and three unablated corneas) were topically treated with 50 μL of fluorescently labeled siRNA complexed with nanoparticles for 1 minute using a vacuum trephine while the corneas in FL-siRNA group (three ablated corneas) received an equivalent dose of FL-siRNA without NP. The corneas were cultured for 6 hours and then collected for histology. A mosaic was created from several consecutive confocal images to give an overall perspective of the wounding region of the cornea.

2.3.3 Experiment 3—Experiment 3 was designed to assess the relative levels of corneal haze that developed in excimer-ablated corneas, and to determine if the level of corneal haze could be reduced by treatment with a steroid (prednisolone acetate) that is commonly used to reduce corneal inflammation or by treatment with a NP-siRNA formulation that targeted three key scar-stimulating genes (TGFB1, TGFBR2 and CTGF). The experiment included four groups of corneas: unablated, ablated & untreated, ablated & treated with NP-siRNA, and ablated & treated with prednisolone acetate. Six corneas were cultured in each of the four groups. After excimer laser ablation, all the corneas were cultured in DMEM supplemented with 1 ng/ml of TGFB1 and 1% antibiotic solution and the media was changed every 2 days. Furthermore, one group of four corneas were treated with 2 drops of 1%prednisolone acetate ophthalmic suspension (Pacific Pharma) and another set of four corneas were treated with the triple siRNA combination delivered using NP for the first three days after ablation. After 14 days of culture, corneas were photographed then returned to culture, until on day 21, three corneas of each test group were independently processed for qRT-PCR for measurement of SMA mRNA. The remaining three corneas in each group were processed for immunohistostaining of SMA protein.

2.4 Reverse Transcription–Polymerase Chain Reaction

Total RNA was extracted using the Qiagen RNeasy mini isolation kit (Qiagen, Inc., Valencia, CA) and used according to the manufacturer's directions. cDNA was synthesized using the High Capacity cDNA Reverse Transcription Kit (Applied Biosytems, Carlsbad, CA) according to manufacturer's procedure. The level of mRNA for TGFB1, CTGF, TGFBR2, SMA, collagen II, and 18S ribosomal RNA were determined using the Real-Time PCR TaqMan assay. The primers and probes for each gene are defined in Table A1. The endogenous control, ribosoma18S RNA, was used normalize target genes. Primers, probes and cDNA were combined with TaqMan Universal PCR Master Mix (Applied Biosytems, Carlsbad, CA) and amplification was performed by the Applied Biosystems 7300HT Fast Real Time PCR System (Carlsbad, CA). The thermal cycling conditions were as follows: 2 min at 50°C, 10 min at 95°C, 40 cycles of 15 sec at 95°C, and 1 min at 60°C. The relative gene expression of the growth factors was calculated using the 2-ΔΔCt method.

2.5 Immunohistochemistry

Corneas from the experiment assessing delivery of the fluorescein-labeled siRNA-nanoparticle formulation were collected 6 hours after transfection. Corneas from the therapeutic experiment were cultured for 21 days before collection and fixing. To stain for

SMA, the rabbit corneas from the both the experiments were fixed overnight in 4 % paraformaldehyde. They were then bisected, embedded in Optimal Cutting Temperature medium (OCT) (Sakura Finetek) then 10 μm thick sections were cut and collected on glass slides. The slides were then washed with PBS and blocked in horse serum for 1 hour. Finally, sections were incubated with SMA antibody-Cy3 (Sigma) for 1hour at room temperature. The slides were mounted with DAPI and imaged using confocal and fluorescence microscopes.

2.6 Scar Imaging

A Nikon D7000 digital camera was outfitted with a macro lens capable of native 1:1 reproduction (60mm Nikkor) and the Nikon R1C1 Creative Lighting System (CLS) flash system. The D7000 was set to the “Standard” program, ISO 100, manual exposure with a shutter speed of 1/250 second and f/57. Shutter speed is the amount of time the shutter in the camera remains open. A high shutter speed would greatly reduce the amount of ambient light entering the camera. The aperture of the camera is given by the f-stop value (f/57). Smaller the aperture, lesser would be the amount of light entering the camera. To visualize and measure haze, the lens was outfitted with a circular ring flash whose flash power was set manually (1/6th D7000) and neither the flash nor lens had a filter. For all images, the lens was set to manual focus and pre-focused to a 1:1 reproduction ratio, and the camera was fixed to a tripod and focused by moving the camera closer or further from the subject. Guide lights on the flash heads were used to facilitate haze visualization and focusing.

Hence, with this current set up the object is exclusively illuminated by the circular ring flash outfitted to the camera. Increasing the shutter speed won't affect the flash exposure because it is of much shorter duration than that of the shutter speed. In other words, the image of the cornea obtained in this study is illuminated only by the flash and would be the same if imaged in a dark or a well-lit room.

2.7 Image Analysis

To improve the contrast of scar formation in the ablated regions of the cornea, the native full color images were converted to grey scale. This was followed by reducing the background light scattering observed in unablated regions of the cornea to a minimum. The background from the unablated regions of the cornea was not set to any user-derived value. Instead, the ‘set black point’ option from Adobe Photoshop was used for background correction. In this method, an area outside the ablated region without any visual signs of haze was set to be black using the ‘set black point’ option. This sample area is used a reference point and set as black. The grey values of all other areas are also accordingly reduced based on this reference point. All processing steps were done globally on the entire image and not locally on any specific area of the image. These steps help in effectively blocking the noise associated with the light scattering of unablated regions, which enables the finer details of the scar to be discerned. Hence, instead of having a specific set of brightness and contrast values for each picture, the scarring regions in the corneas were normalized to their respective unablated and unscarred regions. The ablation regions in these processed images were then selected with the lasso tool and percent haze was calculated by measuring the pixel intensity in these selected regions.

2.8 Statistical Analysis

All experiments were performed in triplicate and all statistical analyses were conducted using GraphPad prism (San Diego, CA). Student's t-test or Analyses of Variances (ANOVA) with Tukey's post-hoc assessments were used accordingly to test for significance between the groups. Results were considered statistically significant where $p<0.05$.

3. RESULTS

Using rabbit corneas cultured at the air-liquid interface, we analysed the ability of the laser ablation to produce a scar-like response in corneas cultured *ex vivo*. Scarring was evaluated in terms of specific markers of wound healing (expression of pro-fibrotic genes) and transparency (pixel intensity of scarring regions in the ablated region). Further, to evaluate the efficacy of this system as a therapeutic testing model, we evaluated the ability of prednisolone and nanoparticle (NP) complexed with three siRNAs directed at three key scarring genes, TGFB1, TGFBR2, and CTGF, in reducing the formation of these scar-like features.

3.1 *Ex vivo* cultured corneas that were ablated develop scar-like features

Corneas of freshly obtained rabbit globes were ablated with an excimer laser to a depth of 155 μm to create a 6 mm diameter central wound then cultured at the air-liquid interface for 21 days in serum free media that was supplemented with 1ng/ml of TGF-B1. After 14 days, the unablated corneas were transparent and showed no signs of any scar-like features while the ablated corneas without any treatment had the most visible scar-like formations in the wounding region (Figure 1- a, b).

3.2 Visual comparison of corneas treated with therapeutic agents

Figure 2 shows processed digital images of the corneas from all the treatment groups in Figure 1. Ablated corneas without any treatment (positive scarring control) developed the most robust scar-like features, while corneas treated with NP-siRNA or treated with steroid developed markedly less scar-like features that were readily apparent by simple visual examination. Unablated cornea did not develop any haze-like features and was used as a negative control.

3.3 Comparison of RNA level expression of pro-fibrotic genes in ablated and unablated corneas

Levels of expression of pro-fibrotic genes in unablated and ablated corneas cultured in full serum conditions without any treatment were assessed by qRT-PCR. RNA from the central scar-like tissue was collected using an 8 mm punch biopsy, and the expression levels of 5 pro-fibrotic genes were analyzed using qRT-PCR. The levels of RNA for all five pro-fibrotic genes were higher in the ablated corneas when compared to the unablated corneas (Figure 3). In particular, the expression of TGFB1 and SMA were 8 and 4 fold higher, respectively, in injured corneas.

3.4 Delivery of siRNA by nanoparticles

The efficacy of the delivery of nanoparticles complexed with siRNA to different layers of the cornea was assessed by detecting the presence of a fluorescently labelled scrambled siRNA sequence in histology sections of treated corneas. In ablated corneas treated with nanoparticle complexed fluorescently labelled siRNA (NP-FL-siRNA), a fluorescence gradient was observed. The anterior stromal layers directly beneath the area where the NP-FL-siRNA was applied using a vacuum trephine had a high fluorescence intensity. The intensity of fluorescence progressively decreased with increasing distance from the anterior surface. Higher magnification images of the sections show uptake of siRNA by the cells (Figure 4 a–c). No fluorescence was observed in the stroma of excimer-ablated corneas when FL-siRNAs alone were applied (Figure 4c). Also, only a few superficial epithelial cells were fluorescent when FL-NP- siRNAs were applied to the intact unablated cornea (Figure 4b). Neither the stroma layers nor the endothelial cell layer were fluorescent.

3.5 Treatment with NP-siRNA or steroid reduce haze formation

The contrast-enhanced images of three replicate corneas from each of the four treatment groups were used to measure the percentage of haze formed (Supplemental Figures 1 – 4). The ablated regions in these processed images were selected with the lasso tool and percent haze was calculated by measuring the pixel intensity in these selected regions (Image 5, panels a &, b). The pixel intensity in this selected region should be lower in the unablated corneas due to their relatively high transparency, while the intensity of these regions in ablated corneas should be higher in corneas with ”scar” depending on the severity of the haze. The percentage of haze developed in ablated corneas without any siRNA/steroid treatment was 22% (calculated with respect to the unablated corneas which developed no haze). In contrast, treatment of ablated corneas with NP-siRNA improved the transparency of the corneas, resulting in a haze percentage of 9.6% when compared to the unablated corneas. Similarly, treatment of ablated corneas with steroid also improved the transparency of the corneas, resulting in a haze percentage of 7% when compared to the unablated corneas. Therefore, treatment of the ablated corneas with NP-siRNA reduced haze formation by 55%, while treatment with steroids reduced haze formation by 68% compared to the ablated corneas that received no treatment ($p=0.05$).

3.6 Treatment with NP-siRNA or steroid reduce mRNAs for scarring genes

RNA from the scar-like tissue was collected using a 8mm punch biopsy, and the expression levels of SMA were analyzed with qRT-PCR. The SMA expression in the treated corneas (NP-siRNA and steroids) was significantly ($p<0.05$) lower than that of the ablated and untreated corneas (Figure 6a). Specifically, the NP-siRNA treatment was able to reduce the SMA expression by 77%, while the steroid treatment reduced the SMA expression by 85%.

3.7 Immunohistostaining of corneal tissues shows reduction in SMA after treatment with NP-siRNA or steroid

Immunocytochemistry was performed on three corneas from each of the experimental groups to visualize the presence of SMA in the ablated untreated corneas and assess knockdown of SMA protein. Rabbit corneas that were ablated and untreated show intense

SMA staining in the basal epithelium and anterior stroma (Figure 6b). A similar pattern of myofibroblasts containing SMA was observed in both mice and rabbits after a PTK injury. Corneas that were treated with NP-siRNA and steroids showed reduction in staining for SMA when compared to untreated controls (Figure 6c, d).

4. DISCUSSION

Using excimer laser ablated rabbit corneas cultured in an *ex vivo* organ system for up to 21 days, we were able to reproduce the reduction of transparency observed in living rabbits when corneas are subjected to laser injury (Figure 1a, b). Since this model utilizes freshly obtained intact rabbit globes, it is closer to the *in vivo* situation than the three-dimensional cell culture systems reported by other investigators.(Karamichos et al., 2010; Janin-Manificat et al., 2012)

Several *in vitro* organ culture methods have been proposed to study the corneal wound healing processes.(Møller-Pedersen and Møller, 1996; Richard et al.) Air/liquid interface organ cultures have been shown to improve epithelial cell morphology and preserve stromal keratocytes for at least 4 weeks.(Castro-Combs et al., 2008) In addition, our *ex vivo* model system was able to reproduce key aspects of corneal scarring reported *in vivo* for rabbits. Specifically, there was a marked increase in the levels of mRNA expression of five pro-fibrotic genes in the wound tissue. In particular, levels of SMA mRNA and protein, a key marker of corneal scarring, significantly increased when compared to the unablated corneas (Figure 3).

In this culture system, corneal scar formation develops in the absence of an intact immune system, tear secretion, and corneal innervation, which are all known to play important roles in corneal wound healing. This enables this *ex vivo* organ culture model to isolate and study the effects of various molecular pathways that regulate haze formation in the absence of these other processes that influence corneal scarring. This also makes this *ex vivo* system an ideal model to screen large numbers of potential therapeutic agents that target different molecular pathways for reduction of corneal haze formation. In this study, we used a triple siRNA combination targeting TGFB1, TGFBR2 and CTGF all of which have been shown to play an important role in corneal scarring.(Jester et al., 1999; Chen et al., 2000; Blalock et al., 2003) This effective triple siRNA, in *in vitro* knockdown experiments, significantly reduced mRNA levels of target genes (>80%) and downstream scarring genes (>85%), SMA protein (>95%), and significantly reduced cell migration without reducing cell viability. (sriram et al., 2013c)

In the cornea it has been shown that fundamental behaviors of epithelial and stromal cells, including proliferation, adhesion, and migration, are modulated by substratum topography. (Pot et al., 2010) A previous study by Netto et al.(Netto et al., 2006) indicated that larger-scale topographic irregularities caused by corneal surgical intervention contribute to myofibroblast generation and haze formation *in vivo*. It has also been shown that nanoscale topographic features modulate TGFB1-induced myofibroblast differentiation and αSMA expression, possibly through upregulation of Smad7. It is therefore possible that in the wound environment, native nanotopographic cues assist in stabilizing the keratocyte/

fibroblast phenotype while pathologic microenvironmental alterations may be permissive for increased myofibroblast differentiation and the development of fibrosis and corneal haze. (Myrna et al., 2012) Hence, studying anti-fibrotic therapies in excimer laser ablated *ex vivo* corneas is a better system than in cell culture experiments as they provide pathologic microenvironmental alterations similar to *in vivo* conditions that may stimulate the fibroblasts to change to the myofibroblast phenotype.

One of the main challenges in the therapeutic use of siRNA has been the delivery of siRNAs to cells in complex tissues. In this study, we used a histidine and lysine based commercially available nanoparticle kit. In ablated corneas treated with these polycationic nanoparticles complexed with fluorescently labelled siRNA (NP-FL-siRNA), a fluorescence gradient was observed. The anterior stromal layers directly beneath the area where NP-FL-siRNA was applied using a vacuum trephine had a high fluorescence intensity. The intensity of fluorescence progressively decreased with increasing distance from the anterior surface. However, there was an increase in the fluorescence intensity in the endothelial cell layers. These results suggest that, in the absence of an epithelium, the endothelium poses maximum resistance to the penetration of FL-NP-siRNA complex, leading to an increased concentration of the FL-NP-siRNA nanoparticles in this layer. This was also reported by Hämäläinen et al.(Hämäläinen et al., 1997) in which they found the permeability of the central stroma to be higher than that of the endothelium. Importantly, no fluorescence was observed in the stroma of excimer-ablated corneas when FL-siRNAs alone were applied (Figure 4c). Also, only a few superficial epithelial cells were fluorescent when FL-NP-siRNAs were applied to the intact unablated cornea (Figure 4b). Neither the stromal layers nor the endothelial cell layer were fluorescent. These results suggest that the fluorescence pattern observed in corneas when FL-NP-siRNA nanoparticles were applied topically to corneas in the area of epithelial ablation was due to penetration of the FL-NP-siRNA nanoparticles into the stroma and not due to absorption from the media. Overall, these results demonstrated the importance of the polycationic nanoparticle carrier system to enhance deep penetration of the FL-siRNAs into the cornea and uptake by stroma keratocytes and endothelial cells. However, the intact epithelium is still an effective barrier to even the FL-NP-siRNA nanoparticles.

There is currently no standard imaging methodology for quantitatively measuring the extent of corneal haze. The accepted clinical method to evaluate corneal haze is visual grading by an experienced ophthalmologist. However, this method fails to give a definitive quantifiable measurement and also suffers from subjective bias of the observer. Ultrasound biomicroscope (UBM) uses back-scattered signals reflected from different layers of tissues and then reconstructs structural images.(Zhou et al., 2013) In general, the resolution of this technique is not very sensitive to quantify mild haze. It has been reported that haze scores of less than 2 and mild subepithelial haze formation cannot be visualized by Ultrasound biomicroscopy.(Nagy et al., 1996) (Foster et al., 2000) Confocal microscopy allows *in vivo* presentation of corneal structure changes on the cellular level.(Cavanagh et al., 1993) In the field of cornea scarring, it has been predominantly used to visualize light scattering in the cornea and not for quantifying the reduction of haze because of its fair resolution (white light source) and local perspective of the wounding region. These techniques also require

expensive instruments and skilled technicians to image the cornea. The digital camera imaging system to measure corneal haze over the entire ablated region of the cornea described in this study is convenient, accurate, affordable, and can be performed by essentially any vision researcher. In this study, we were able to show that treatment of the ablated corneas with NP-siRNA reduced haze formation by 55%, while treatment with steroids reduced haze formation by 68% when compared to the ablated corneas that received no treatment (Figure 5c). The visual results were confirmed by a high RNA level knockdown of SMA as observed by qRT-PCR (78% by NP-siRNA and 85% by steroids) (Figure 6a).

SMA immunohistostaining of rabbit corneas that were ablated and untreated shows SMA staining in the basal epithelium and anterior stroma (Figure 6). A similar pattern of myofibroblasts formation was observed in both mice and rabbits after a PTK injury. (Nakamura et al., 2001; Netto et al., 2006; Mohan et al., 2008; 2011) In addition, when severe haze develops in human corneas after PRK, it is nearly always localized immediately beneath the epithelium and in the anterior stroma,(Shah et al., 1998; Siganos et al., 1999) which is in the same location that myofibroblasts are noted in the ablated corneas cultured in this *ex vivo* system. Hence, the focus of the data in this study was primarily on these regions and not on the endothelium. However, the endothelia of the corneas used in this model were also viable and undamaged as observed in the clear unablated control corneas, which would have developed haze if the endothelial layer was extensively damaged. Corneas that were treated with NP-siRNA and steroids show reduced staining for SMA without any damage to the different layers, showing protein level knockdown of both the treatments.

There currently are no FDA approved drugs that selectively reduce the expression of genes causing corneal scarring and haze. Mitomycin C is used during some ocular surgeries, but it may have very damaging side effects, including death of endothelial cells, (Sihota et al., 1998) stromal melting, and conjunctival thinning. (Morales et al., 2006). Corticosteroids like prednisolone acetate used in this experiment, have also been used as potential anti-fibrotic agents. Studies have shown that although corticosteroids have been demonstrated to reduce corneal haze in some cases, there are a number of severe side effects to this treatment including cataract and risk of glaucoma after prolonged use. (Carnahan and Goldstein, 2000) Thus, there is a need for an effective anti-scarring drug that can be given topically and specifically targets fibrotic genes while also avoiding non-specific serious side effects that threaten vision. In addition, using a combination of siRNAs that target three key genes in a dominant scarring pathway created an enhanced knockdown effect compared to a single siRNA targeting only one gene product (sriram et al., 2013b).

Animal models have been used for corneal scarring studies post excimer laser surgery.(Netto et al., 2006; Mohan et al., 2008; 2011) However, their use in large scale is limited for practical reasons. Results from this study show that the development of corneal haze in the *ex vivo* cultured corneas in terms of markers of corneal scarring is very similar to that observed in animals. Studies have also shown enucleated rabbit eyes sustained in culture retain wound healing dynamics and are comparable to live rabbit eye model in terms of laser radiation exposure.(McCally et al., 1992; McCally and Bargeron, 2000; Kabosova et al., 2003; Fyffe, 2005) The use of this *ex vivo* organ culture can help reduce the need for

animals in experiments.(Toropainen, 2007). The *ex vivo* scarring model can be an important aid for screening and optimization of new anti-scarring drugs in addition to it being an important tool to study and understand the molecular pathways of the corneal wound healing process.

Supplementary Material

Refer to Web version on PubMed Central for supplementary material.

Acknowledgments

Supported by Grants from the U.S. Army Medical Research Acquisition Activity W81XWH-10-2-0917, National Eye Institute grant EY000587, National Eye Institute T32-EY07132 training grant, and the National Eye Institute P30-EY021721 Vision Core Grant,

References

Blalock TD, Duncan MR, Varela JC, Goldstein MH, Tuli SS, Grotendorst GR, Schultz GS. Connective tissue growth factor expression and action in human corneal fibroblast cultures and rat corneas after photorefractive keratectomy. Invest Ophthalmol Vis Sci. 2003; 44:1879–1887. [PubMed: 12714619]

Borisy AA, Elliott PJ, Hurst NW, Lee MS, Lehar J, Price ER, Serbedzija G, Zimmermann GR, Foley MA, Stockwell BR. Systematic discovery of multicomponent therapeutics. Proc Natl Acad Sci USa. 2003; 100:7977–7982. [PubMed: 12799470]

Carnahan MC, Goldstein DA. Ocular complications of topical, peri-ocular, and systemic corticosteroids. Curr Opin Ophthalmol. 2000; 11:478–483. [PubMed: 11141645]

Carrington LM, Albon J, Anderson I, Kamma C, Boulton M. Differential regulation of key stages in early corneal wound healing by TGF-beta isoforms and their inhibitors. Invest Ophthalmol Vis Sci. 2006; 47:1886–1894. [PubMed: 16638995]

Castro-Combs J, Noguera G, Cano M, Yew M, Gehlbach PL, Palmer J, Behrens A. Corneal wound healing is modulated by topical application of amniotic fluid in an ex vivo organ culture model. Exp Eye Res. 2008; 87:56–63. [PubMed: 18555991]

Cavanagh HD, Petroll WM, Alizadeh H, He YG, McCulley JP, Jester JV. Clinical and diagnostic use of in vivo confocal microscopy in patients with corneal disease. Ophthalmology. 1993; 100:1444–1454. [PubMed: 8414403]

Chen C, Michelini-Norris B, Stevens S, Rowsey J, Ren X, Goldstein M, Schultz G. Measurement of mRNAs for TGFss and extracellular matrix proteins in corneas of rats after PRK. Invest Ophthalmol Vis Sci. 2000; 41:4108–4116. [PubMed: 11095603]

Chou ST, Leng Q, Scaria P, Woodle M, Mixson AJ. Selective modification of HK peptides enhances siRNA silencing of tumor targets in vivo. Cancer Gene Therapy. 2011; 18:707–716. [PubMed: 21818135]

Chou TC, Talalay P. Analysis of combined drug effects: a new look at a very old problem. Trends in Pharmacological Sciences. 1983

Chuck RS, Behrens A, Wellik S, Liaw LLH, Dolorico AMT, Sweet P, Chao LC, Osann KE, McDonnell PJ, Berns MW. Re-epithelialization in Cornea Organ Culture After Chemical Burns and Excimer Laser Treatment. Arch Ophthalmol. 2001a; 119:1637–1642. [PubMed: 11709014]

Chuck RS, Behrens A, Wellik SR, Liaw LH, Sweet PM, Osann KE, McDonnell PJ, Berns MW. Simple organ cornea culture model for re-epithelialization after in vitro excimer laser ablation. Lasers Surg Med. 2001b; 29:288–292. [PubMed: 11573233]

Edwards A, Prausnitz MR. Predicted Permeability of the Cornea to Topical Drugs. Pharmaceutical Research. 2001; 18:1497–1508. [PubMed: 11758755]

Eraslan M, Toker E. Mechanisms of corneal wound healing and its modulation following refractive surgery. Marmara Med J. 2009; 22:169–178.

Foster FS, Pavlin CJ, Harasiewicz KA, Christopher DA, Turnbull DH. Advances in ultrasound biomicroscopy. Ultrasound in Medicine & Biology. 2000; 26:1–27. [PubMed: 10687788]

Fyffe, JG. Corneal Injury to Ex-Vivo Eyes Exposed to a 3.8 Micron Laser. 2005.

Grimm D. Small silencing RNAs: state-of-the-art. Adv Drug Deliv Rev. 2009; 61:672–703. [PubMed: 19427885]

Hämäläinen KM, Kananen K, Auriola S, Kontturi K, Urtti A. Characterization of paracellular and aqueous penetration routes in cornea, conjunctiva, and sclera. Invest Ophthalmol Vis Sci. 1997; 38:627–634. [PubMed: 9071216]

Janin-Manificat H, Rovère M-R, Galiacy SD, Malecaze F, Hulmes DJS, Moali C, Damour O. Development of ex vivo organ culture models to mimic human corneal scarring. Mol Vis. 2012; 18:2896–2908. [PubMed: 23233791]

Jester JV, Barry-Lane PA, Cavanagh HD, Petroll WM. Induction of alpha-smooth muscle actin expression and myofibroblast transformation in cultured corneal keratocytes. Cornea. 1996; 15:505–516. [PubMed: 8862928]

Jester JV, Petroll WM, Cavanagh HD. Corneal stromal wound healing in refractive surgery: the role of myofibroblasts. Prog Retin Eye Res. 1999; 18:311–356. [PubMed: 10192516]

Kabosova A, Kramerov AA, Aoki AM, Murphy G, Zieske JD, Ljubimov AV. Human diabetic corneas preserve wound healing, basement membrane, integrin and MMP-10 differences from normal corneas in organ culture. Exp Eye Res. 2003; 77:211–217. [PubMed: 12873452]

Karamichos D, Guo XQ, Hutcheon AEK, Zieske JD. Human corneal fibrosis: an in vitro model. Invest Ophthalmol Vis Sci. 2010; 51:1382–1388. [PubMed: 19875671]

Keith CT, Borisy AA, Stockwell BR. Multicomponent therapeutics for networked systems. Nat Rev Drug Discov. 2005; 4:71–78. [PubMed: 15688074]

Kim D-H, Behlke MA, Rose SD, Chang M-S, Choi S, Rossi JJ. Synthetic dsRNA Dicer substrates enhance RNAi potency and efficacy. Nat Biotechnol. 2005; 23:222–226. [PubMed: 15619617]

Kleinman ME, Yamada K, Takeda A, Chandrasekaran V, Nozaki M, Baffi JZ, Albuquerque RJC, Yamasaki S, Itaya M, Pan Y, et al. Sequence- and target-independent angiogenesis suppression by siRNA via TLR3. Nature. 2008; 452:591–597. [PubMed: 18368052]

la Fuente de M, Seijo B, Alonso MJ. Bioadhesive hyaluronan–chitosan nanoparticles can transport genes across the ocular mucosa and transfect ocular tissue. Gene Ther. 2008; 15:668–676. [PubMed: 18305575]

Lee VH, Robinson JR. Topical ocular drug delivery: recent developments and future challenges. J Ocul Pharmacol. 1986; 2:67–108. [PubMed: 3332284]

Liang L, Sheha H, Li J, Tseng SCG. Limbal stem cell transplantation: new progresses and challenges. Eye (Lond). 2009; 23:1946–1953. [PubMed: 19098704]

McCally, RL.; Bargeron, CB. Corneal Damage from Infrared Radiation. 2000.

McCally RL, Farrell RA, Bargeron CB. Cornea epithelial damage thresholds in rabbits exposed to Tm:YAG laser radiation at 2.02 microns. Lasers Surg Med. 1992; 12:598–603. [PubMed: 1453860]

Mohan RR, Stapleton WM, Sinha S, Netto MV, Wilson SE. A novel method for generating corneal haze in anterior stroma of the mouse eye with the excimer laser. Exp Eye Res. 2008; 86:235–240. [PubMed: 18068702]

Mohan RR, Tandon A, Sharma A, Cowden JW, Tovey JCK. Significant Inhibition of Corneal Scarring In Vivo with Tissue-Selective, Targeted AAV5 Decorin Gene Therapy. Invest Ophthalmol Vis Sci. 2011; 52:4833–4841. [PubMed: 21551414]

Morales AJ, Zadok D, Mora-Retana R, Martínez-Gama E, Robledo NE, Chayet AS. Intraoperative mitomycin and corneal endothelium after photorefractive keratectomy. Am J Ophthalmol. 2006; 142:400–404. [PubMed: 16935583]

Myrna KE, Mendonsa R, Russell P, Pot SA, Liliensiek SJ, Jester JV, Nealey PF, Brown D, Murphy CJ. Substratum topography modulates corneal fibroblast to myofibroblast transformation. Invest Ophthalmol Vis Sci. 2012; 53:811–816. [PubMed: 22232431]

Møller-Pedersen T. Keratocyte reflectivity and corneal haze. Exp Eye Res. 2004; 78:553–560. [PubMed: 15106935]

Møller-Pedersen T, Møller HJ. Viability of human corneal keratocytes during organ culture. Acta Ophthalmol Scand. 1996; 74:449–455. [PubMed: 8950392]

Nagy ZZ, Németh J, Sûveges I, Csákány B. Examination of subepithelial scar formation after photorefractive keratectomy with the ultrasound biomicroscope. Klin Monbl Augenheilkd. 1996; 209:283–285. [PubMed: 9044975]

Nakamura K, Kurosaka D, Bissen-Miyajima H, Tsubota K. Intact corneal epithelium is essential for the prevention of stromal haze after laser assisted in situ keratomileusis. Br J Ophthalmol. 2001; 85:209–213. [PubMed: 11159488]

Netto MV, Mohan RR, Sinha S, Sharma A, Dupps W, Wilson SE. Stromal haze, myofibroblasts, and surface irregularity after PRK. Exp Eye Res. 2006; 82:788–797. [PubMed: 16303127]

Pellegrini G, Rama P, Mavilio F, De Luca M. Epithelial stem cells in corneal regeneration and epidermal gene therapy. J Pathol. 2009; 217:217–228. [PubMed: 18855878]

Pot SA, Liliensiek SJ, Myrna KE, Bentley E, Jester JV, Nealey PF, Murphy CJ. Nanoscale topography-induced modulation of fundamental cell behaviors of rabbit corneal keratocytes, fibroblasts, and myofibroblasts. Invest Ophthalmol Vis Sci. 2010; 51:1373–1381. [PubMed: 19875665]

Reynolds A, Anderson EM, Vermeulen A, Fedorov Y, Robinson K, Leake D, Karpilow J, Marshall WS, Khvorova A. Induction of the interferon response by siRNA is cell type- and duplex length-dependent. Rna. 2006; 12:988–993. [PubMed: 16611941]

Richard, NR.; Anderson, JA.; Weiss, JL.; Binder, PS. Air/liquid corneal organ culture: a light microscopic study. Informahealthcare.com

Saghizadeh M, Epifantseva I, Hemmati DM, Ghiam CA, Brunken WJ, Ljubimov AV. Enhanced wound healing, kinase and stem cell marker expression in diabetic organ-cultured human corneas upon MMP-10 and cathepsin F gene silencing. Invest Ophthalmol Vis Sci. 2013; 54:8172–8180. [PubMed: 24255036]

Sakimoto T, Rosenblatt MI, Azar DT. Laser eye surgery for refractive errors. Lancet. 2006; 367:1432–1447. [PubMed: 16650653]

Sasaki H, Yamamura K, Nishida K, Nakamura J, Ichikawa M. Delivery of drugs to the eye by topical application. Prog Retin Eye Res. 1996; 15:583–620.

Shah SS, Kapadia MS, Meisler DM, Wilson SE. Photorefractive keratectomy using the summit SVS Apex laser with or without astigmatic keratotomy. Cornea. 1998

Siganos DS, Katsanevaki VJ, Pallikaris IG. Correlation of subepithelial haze and refractive regression 1 month after photorefractive keratectomy for myopia. J Refract Surg. 1999; 15:338–342. [PubMed: 10367577]

Sihota R, Sharma T, Agarwal HC. Intraoperative mitomycin C and the corneal endothelium. Acta Ophthalmol Scand. 1998; 76:80–82. [PubMed: 9541440]

Siolas D, Lerner C, Burchard J, Ge W, Linsley PS, Paddison PJ, Hannon GJ, Cleary MA. Synthetic shRNAs as potent RNAi triggers. Nat Biotechnol. 2005; 23:227–231. [PubMed: 15619616]

sriram S, Gibson D, Robinson P, Tuli S, Lewin AS, Schultz G. Reduction of corneal scarring in rabbits by targeting the TGFB1 pathway with a triple siRNA combination. Advances in Bioscience and Biotechnology. 2013a; 04:47.

sriram S, Robinson P, Pi L, Lewin AS, Schultz G. Triple combination of siRNAs targeting TGFβ1, TGFβR2, and CTGF enhances reduction of collagen I and smooth muscle actin in corneal fibroblasts. Invest Ophthalmol Vis Sci. 2013b; 54:8214–8223. [PubMed: 24282226]

Tandon A, Tovey JCK, Sharma A, Gupta R, Mohan RR. Role of transforming growth factor Beta in corneal function, biology and pathology. Curr Mol Med. 2010; 10:565–578. [PubMed: 20642439]

Tanelian DL, Bisla K. A new in vitro corneal preparation to study epithelial wound healing. Invest Ophthalmol Vis Sci. 1992; 33:3024–3028. [PubMed: 1399406]

Tong Y-C, Chang S-F, Liu C-Y, Kao WWY, Huang CH, Liaw J. Eye drop delivery of nano-polymeric micelle formulated genes with cornea-specific promoters. J Gene Med. 2007; 9:956–966. [PubMed: 17724775]

Toropainen, E. Corneal Epithelial Cell Culture Model for Pharmaceutical Studies. 2007.

Zhou SY, Wang CX, Cai XY, Huang D, Liu YZ. Optical coherence tomography and ultrasound biomicroscopy imaging of opaque corneas. Cornea. 2013; 32:e25–e30. [PubMed: 23073488]

6. Appendix

Table A1

TAQMAN™ RT PCR Primers and probe sequences

Growth Factor	Type	Sequences
CTGF	Forward	AGGAGTGGGTGTGTGATGAG
	Reverse	CCAAATGTGTCTTCCAGTCG
	Probe	ACCACACCGTGGTTGGCCCT
TGFβR2	Forward	CGTCGAGACTCCATCTCAAA
	Reverse	AAACAGCCCACAAATGTCAA
	Probe	TCAGCTTTGCACAAGGGCCCT
TGFβ1	Forward	CCTGTACAACCAGCACAACC
	Reverse	CGTAGTACACGATGGGCAGT
	Probe	CTCCAGCGCCTGTGGCACAC
Collagen-I	Forward	TTCTGCAGGGCTCCAATGAT
	Reverse	TCGACAAGAACAGTGTAAGTGAACCT
	Probe	TTGAACTTGTTGCCGAGGGCAACAG
SMA	Forward	AGAGCGCAAATACTCCGTCT
	Reverse	CCTGTTTGCTGATCCACATC
	Probe	CGGCTCCATCCTGGCCTCTC
18S rRNA	Forward	GCCGCTAGAGGTGAAATTCTTG
	Reverse	CATTCTTGGCAAATGCTTTCG
	Probe	ACCGGCGCAAGACGGACCAG

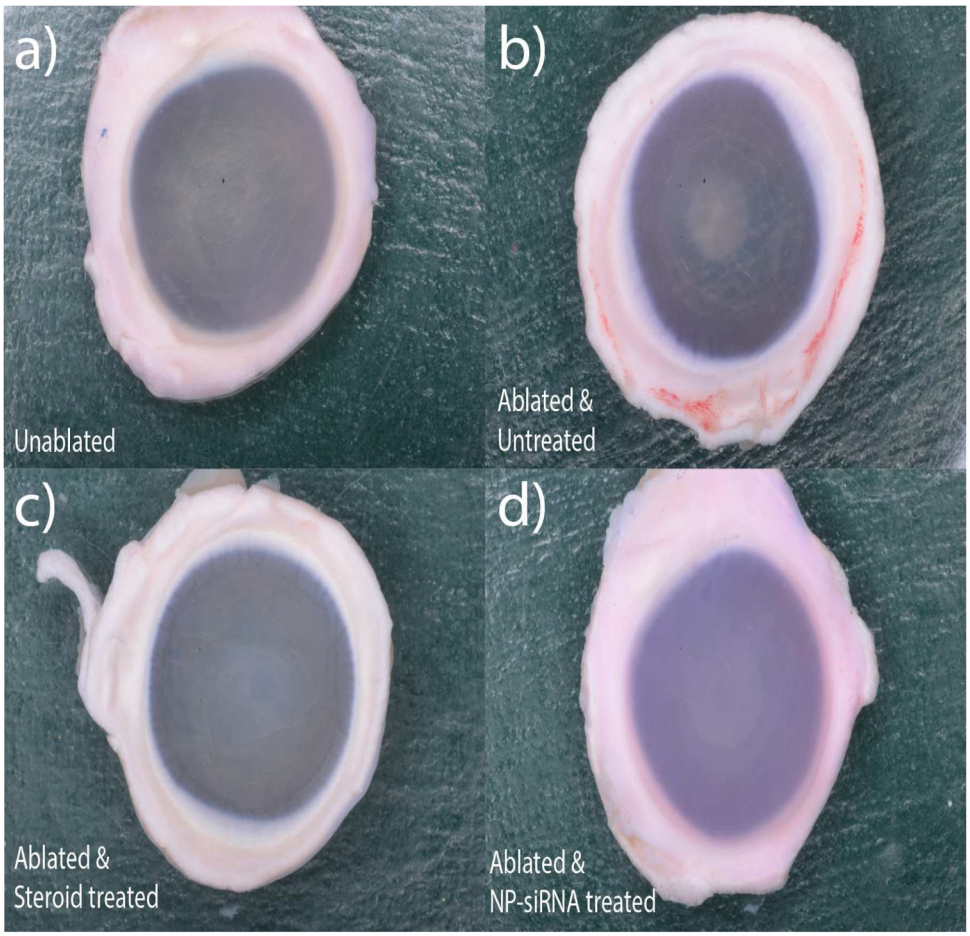

Figure 1. Visual comparison of ablated, unablated and treated corneas

Freshly obtained rabbit globes were ablated to a depth of 155μm and cultured at the air-liquid interface for 14 days in serum free media supplemented with 1ng/ml of TGFB1. Four groups with six corneas each were tested experimentally – a) Unablated corneas, b) Laser ablated with no treatment, c) Laser ablated and treated with Steroids, d) Laser ablated and treated with triple siRNA complexed with nanoparticles.

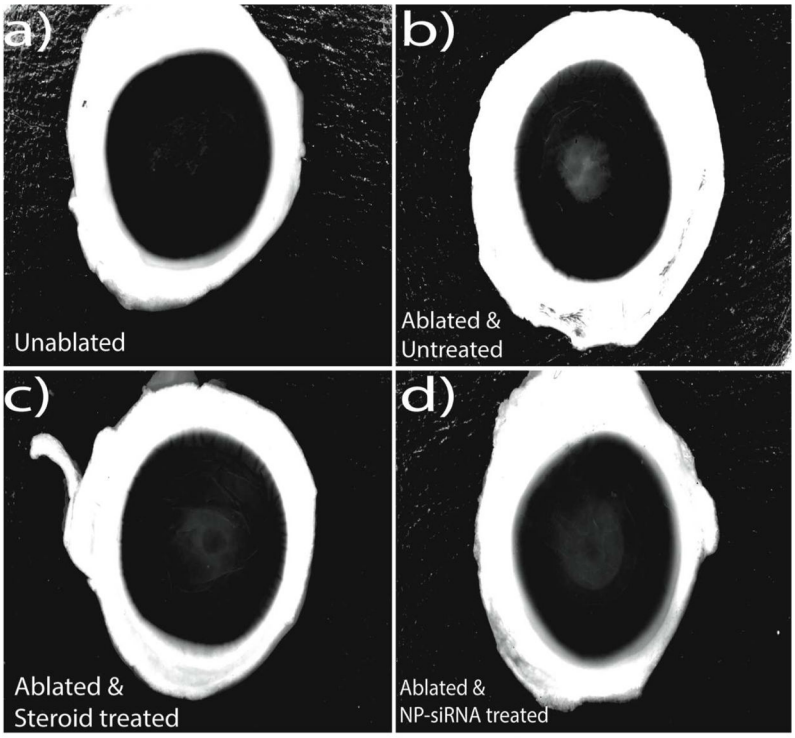

Figure 2. Image analysis of ablated, unablated and treated corneas

The images of corneas from the four groups of the above experiment – a) Unablated corneas, b) Laser ablated with no treatment, c) Laser ablated and treated with Steroids, d) Laser ablated and treated with triple siRNA complexed with nanoparticles were processed with Adobe photoshop to increase the visual contrast of haze. All the images were initially converted to grey scale, which was then followed by background correction to reduce the noise associated with the light scattering of unablated regions.

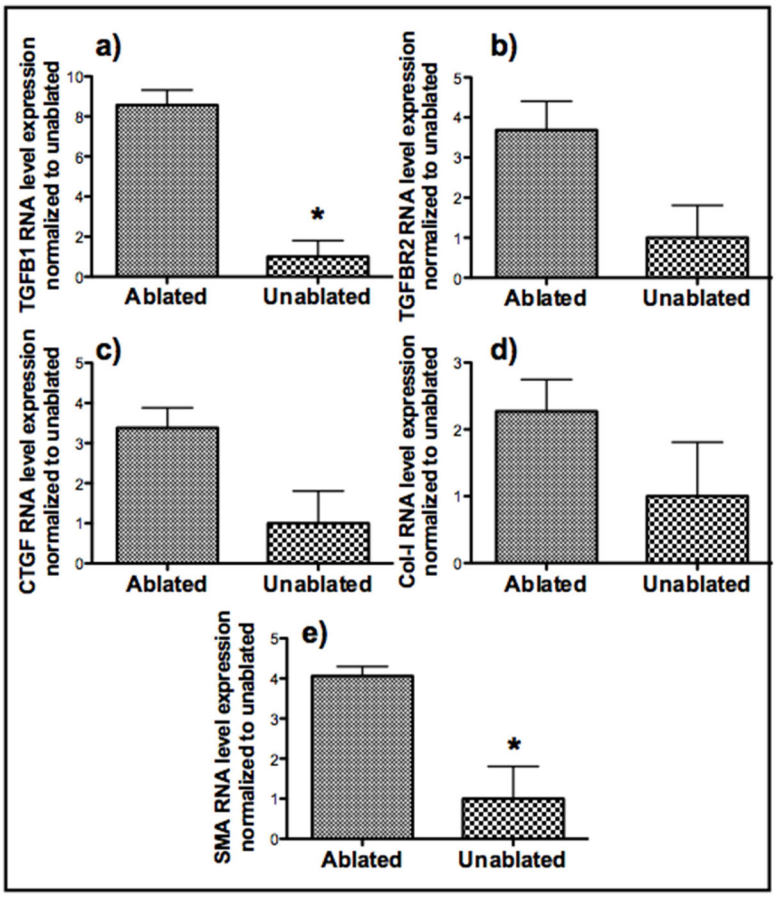

Figure 3. Comparison of RNA level expression of Five pro-fibrotic genes in ablated and unablated corneas

Freshly obtained rabbit globes were ablated to a depth of 155μm and cultured at the air-liquid interface for 14 days in full serum media. RNA from the scar-like tissue was collected using a 8 mm punch biopsy and the expression levels of 5 profibrotic genes were analyzed using qRT PCR. 18S rRNA was used as the housekeeping gene. All RNA expressions were normalized to their respective levels in unablated corneas (n=3 for each group). Asterisks indicate significant differences ($p<0.05$).

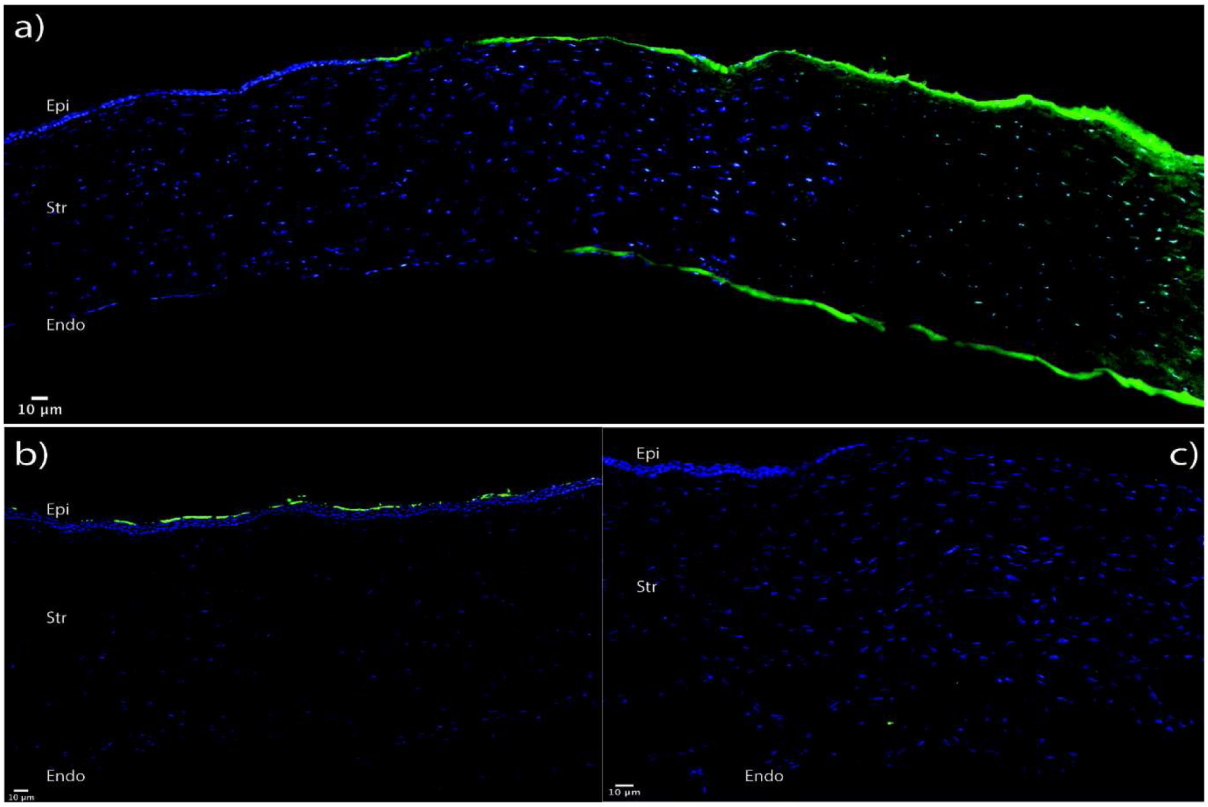

Figure 4. Nanoparticles deliver siRNA to all layers of ablated corneas in organ-culture

Whole rabbit globes were ablated to 125 microns using an excimer laser and treated with fluorescently labeled scrambled siRNA complexed with a nanoparticle for 1 minute. 6 hours after transfection, the corneas were fixed overnight in 4 % paraformaldehyde. They were then bisected, embedded in OCT and then sectioned in 10μm slides. The blue color shows the cell nuclei, which were stained with DAPI, and the green shows the fluorescence of the delivered scrambled siRNA. Image a shows the delivery of siRNA by nanoparticles after ablation. No fluorescence is observed when - b) globes were treated with nanoparticles complexed with siRNAs without ablating the epithelium, c) globes were treated with siRNAs alone without nanoparticles after ablation.

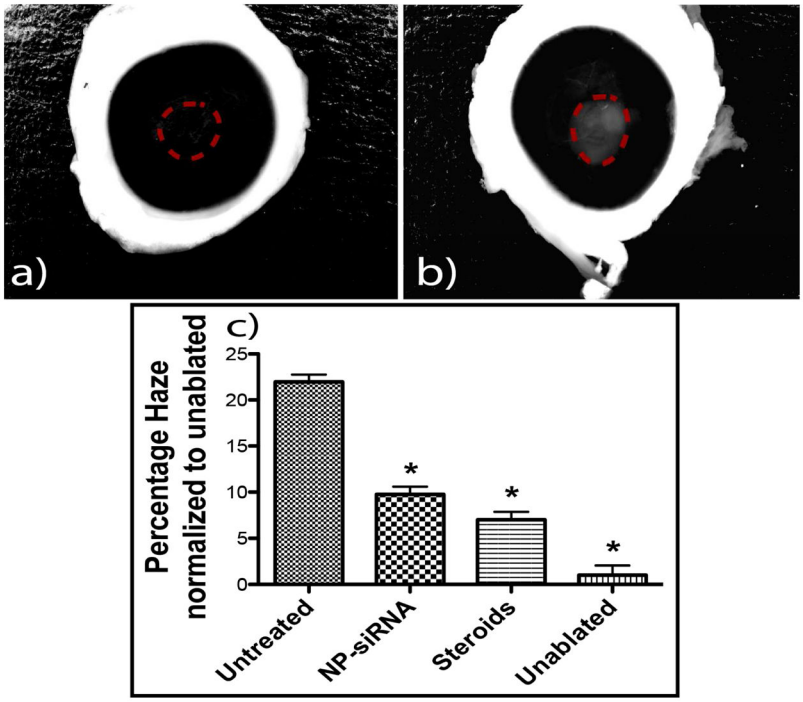

Figure 5. Evaluating the reduction in haze formation

The processed images from Figure 2 were analyzed using Adobe Photoshop to quantify the amount of haze formation. The lasso tool in Photoshop was used to trace the area of the scarring region as shown in images a) and b). Percent haze is calculated by measuring the pixel intensity in these selected regions and normalizing it to area of the selected regions. Image c shows the percentage of haze expressed in the ablated corneas in terms of the unablated corneas. Asterisks indicate significant differences ($p<0.05$) of the experimental group compared to untreated corneas, calculated using ANOVA with Tukey's HSD with n=3 in each experimental group.

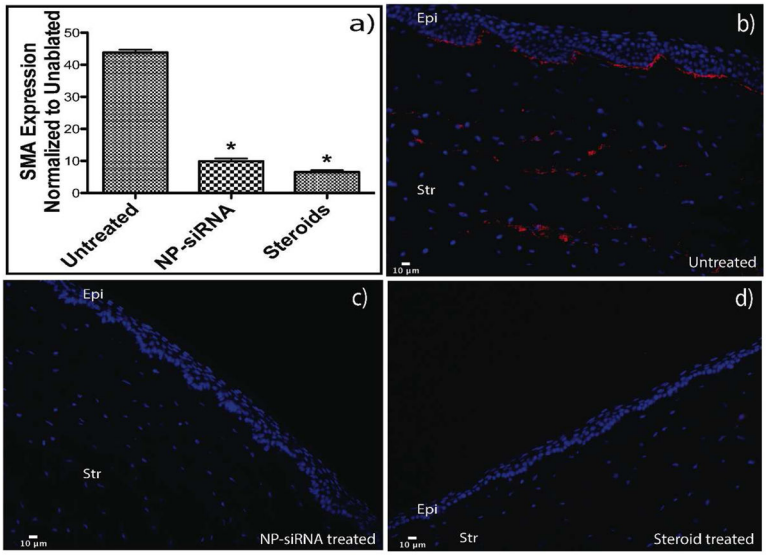

Figure 6. RNA analysis and Immunohistostaining of corneal tissues show reduction in SMA after treatment with steroids and NP-siRNA

RNA from the scar-like tissue was collected using a 8mm punch biopsy and the expression levels of SMA were analyzed with qRT PCR. 18S rRNA was used as the housekeeping gene and all expression levels were normalized to their respective levels in unablated corneas. Image a shows the reduction in SMA expression in treated corneas when compared to the ablated corneas. For immunohistostaining, corneas from the experimental groups were fixed overnight in 4 % paraformaldehyde. They were then bisected, embedded in OCT and then sectioned in 10μm slides. To stain for SMA, slides were blocked in horse serum and then incubated with cy3 labeled SMA antibody. Rabbit globes that were ablated and untreated show SMA staining in the basal epithelium and stroma (Figure a). Figure b) and c) show higher magnification of areas with myofibroblasts. Globes that were ablated and treated with NP-siRNA and steroids show no SMA staining (Figures d and e).